Correlation between Spin−Orbital Coupling and the Superparamagnetic Properties in Magnetite and Cobalt Ferrite Spinel Nanocrystals

Qing Song[§] and Z. John Zhang*

School of Chemistry and Biochemistry, Georgia Institute of Technology, Atlanta, Georgia 30332-0400

Received: January 26, 2006; In Final Form: April 20, 2006

The superparamagnetic properties of $CoFe_2O_4$ and Fe_3O_4 nanocrystals have been systematically investigated. The observed blocking temperature of $CoFe_2O_4$ nanocrystals is at least 100 deg higher than that of the same sized Fe_3O_4 nanocrystals. The coercivity of $CoFe_2O_4$ nanocrystals at 5 K is over 50 times higher than the same sized Fe_3O_4 nanocrystals. The drastic difference in superparamagnetic properties between the similar sized spherical $CoFe_2O_4$ and Fe_3O_4 (or $FeFe_2O_4$) spinel ferrite nanocrystals was correlated to the coupling strength between electron spin and orbital angular momentum ($L-S$) in magnetic cations. Compared to the Fe^{2+} ion, the effect of much stronger spin−orbital coupling at Co^{2+} lattice sites leads to a higher magnetic anisotropy and results in the dramatic discrepancy of superparamagnetic properties between $CoFe_2O_4$ and Fe_3O_4 nanocrystals. These results provide some insight to the fundamental understanding of the quantum origin of superparamagnetic properties. Furthermore, they suggest that it is possible to control the superparamagnetic properties through magnetic coupling at the atomic level in spinel ferrite nanocrystals for various applications.

Introduction

Magnetic nanocrystals have been of great interest over the past several years for the fundamental understanding of nanomagnetism and for their technological applications.[1−3] The magnetic properties of nanocrystals vary greatly with the changing size of the crystals and superparamagnetism is a typical example for such a size-dependent behavior at the nanometer scale. For a wide variety of technical and/or clinical applications, such as magnetic cell sorting and DNA separation,[4−6] contrast enhancement in magnetic resonance imaging (MRI), and site-specific magnetic drug carriers,[7−9] each application requires a somewhat different set of magnetic characteristics in nanocrystals. Therefore, approaches other than varying particle size are essential for controlling magnetic properties to satisfy the requirements in technical and biomedical applications of nanocrystals. Clearly, the systematic studies on the correlations between magnetic properties and the chemical compositions of nanocrystals will generate invaluable insight to the fundamental understanding of magnetic properties, and consequently, enable us to identify suitable candidates of magnetic nanocrystals for various applications, especially in biomedical areas.

The biomedical applications of magnetic nanoparticles have increasingly attracted attentions recently[10] although the interest for such applications was reported even decades ago.[11] Over the years, the magnetic nanoparticles that have been studied in almost all the cases were iron oxides, particularly magnetite (Fe_3O_4).[10−15] This perhaps is primarily due to the result of magnetite being the only magnetic nanoparticles easily available for all these years. Now as a part of the advancement in nanoscience and nanotechnology research over the past decade, new types of magnetic nanocrystals have become available[16−18] and even the quality of magnetite nanocrystals themselves has been greatly improved.[19]

Magnetite ($FeFe_2O_4$) belongs to the crystal family of spinel ferrites, MFe_2O_4 with M = Zn, Mn, Co, Fe, etc. Because of the different strengths of magnetic interactions at lattice sites, the magnetic properties possessed by $CoFe_2O_4$ nanocrystals are very different from magnetite and can be very beneficial to biomedical applications. The systematic and direct comparative studies on these two nanoparticulate systems would provide insights for a better fundamental understanding of the correlations between magnetic properties of nanocrystals and the magnetic couplings at the lattice sites. Consequently, the desirable magnetic properties for biomedical applications can be optimized through chemical manipulation. Since the magnetic properties of nanoparticles are sensitive to the synthesis issues such as method, reaction conditions, and particle size distribution, systematically comparative studies of magnetic properties would be better carried out on high-quality monodispersed magnetite[16] and $CoFe_2O_4$ nanocrystals[20] that have been synthesized under the same reaction conditions.

We here report a quantitative evaluation on the superparamagnetic properties between the same sized spherical cobalt spinel ferrite and magnetite nanocrystals. The nanocrystals have a narrow size distribution (<7%) and have been synthesized under the same reaction conditions. The results show that $CoFe_2O_4$ nanocrystals are at least 100 deg higher in blocking temperature and 50 times larger in coercivity than the same sized Fe_3O_4 nanocrystals. The distinct difference between these two types of spinel ferrite nanocrystals has been correlated to the spin−orbital couplings at Co^{2+} and Fe^{2+} sites. The results suggest that the enhanced magnetic properties make the $CoFe_2O_4$ nanoparticulate system a promising candidate for biomedical applications such as magnetic cell sorting and magnetically guided drug delivery.

Experimental Section

Synthesis of $CoFe_2O_4$ and Fe_3O_4 Nanocrystals. Spherical $CoFe_2O_4$ nanocrystals with sizes from 5 to 13 nm used in this study have been synthesized by a high-temperature nonhydroly-

* To whom correspondence should be addressed. E-mail: zhang@gatech.edu.

§ Present Address: National Renewable Energy Laboratory, 1617 Cole Boulevard, Golden, CO 80401.

10.1021/jp060577o CCC: $33.50
Published on Web 05/20/2006

sis process combined with seed-mediated growth.[20] Spherical Fe_3O_4 nanocrystals with a size range from 4 to 10 nm were produced under the same reaction conditions as $CoFe_2O_4$ nanocrystals. All chemicals were purchased from Aldrich Chemicals Inc. and used without further treatment. To synthesize Fe_3O_4 nanocrystals, a mixture of 20 mL of phenyl ether, 1 mmol of iron(III) acetylacetonate ($Fe(acac)_3$), 5 mmol of 1,2-hexadecanediol, 1 mL of oleic acid, and oleylamine was heated to 260 °C and kept for 30 min. After the solution was cooled to room temperature, 20 mL of ethanol was added and black precipitates were collected by centrifugation. The size of Fe_3O_4 nanocrystals obtained is about 4 nm in diameter. Other sized Fe_3O_4 nanocrystal samples used in this study were prepared by adding these 4 nm Fe_3O_4 nanocrystals as seeds into the above-mentioned solution to grow nanocrystals into a larger size. The size control is through adjusting the molar ratios of seeds to iron precursors in the solution. The as-synthesized nanocrystals were usually washed with hexane and precipitated by acetone alternatively for one or two cycles and the dry samples were stored under vacuum before the magnetic measurements.

Transmission Electron Microscopy. A JEOL JEM 100C operated at 100 kV was used to record transmission electron microscopy (TEM) images and the selected area electron diffraction (SAED) patterns. The samples were prepared by slowly evaporating a drop of nanocrystal suspension in hexane on amorphous carbon-coated copper grids at room temperature.

Magnetic Measurements. Both temperature and magnetic field-dependent magnetization measurements were carried out on a superconducting quantum interference devices (SQUID) magnetometer (Quantum Design MPMS-5S) with a magnetic field up to 5 T. All samples for the magnetic measurements were prepared by fully dispersing an appropriate amount of dry powder nanocrystals in eicosane.

Results and Discussion

The monodispersed Fe_3O_4 nanocrystals with sizes from 4 to 10 nm and $CoFe_2O_4$ nanocrystals with sizes between 5 and 13 nm have been synthesized under the same reaction conditions. The representative TEM images of 10 nm Fe_3O_4 and 12 nm $CoFe_2O_4$ spherical nanocrystals are shown in Figure 1. The measurements of more than 500 individual nanoparticles in TEM micrographs conclude the Fe_3O_4 and $CoFe_2O_4$ nanocrystals have a narrow size distribution of $<7\%$. The crystal structure of both Fe_3O_4 and $CoFe_2O_4$ nanocrystals is cubic spinel, which is determined by the selected area electron diffraction (SAED) and X-ray powder diffraction.

Figure 2 shows the temperature dependence of zero-field-cooling magnetization for Fe_3O_4 and $CoFe_2O_4$ nanocrystals with sizes of 5 and 10 nm. As the temperature increases, the magnetization shows a maximum value at a certain temperature. Afterward, the magnetization begins to decrease and displays a paramagnetic character. The temperature at which the magnetization shows the maximum value is defined as the blocking temperature (T_B). For both Fe_3O_4 and $CoFe_2O_4$ nanocrystals, the blocking temperatures increase as the increasing size of nanocrystals, as shown in Figure 3. However, there is a dramatic discrepancy of blocking temperature for the same sized Fe_3O_4 and $CoFe_2O_4$ nanocrystals. For example, the T_B of 5 nm Fe_3O_4 is about 100 K less than that of 5 nm $CoFe_2O_4$ nanocrystals. Furthermore, such a divergence on the blocking temperature is increasingly larger as the size of nanocrystals increases.

The field-dependent magnetizations at 5 K are presented in Figure 4. The insert displays partial hysteresis curves for 5 and 10 nm Fe_3O_4 nanocrystals at an enlarged scale of field strength

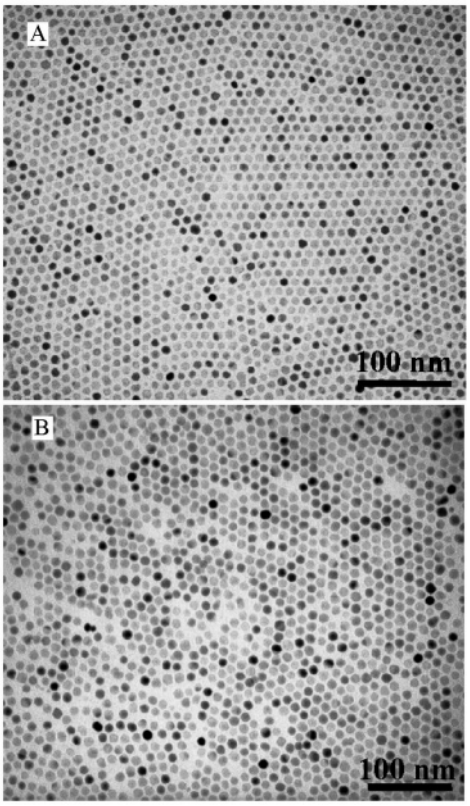

Figure 1. TEM micrographs of 10 nm Fe_3O_4 (panel A) and 12 nm $CoFe_2O_4$ (panel B) nanocrystals.

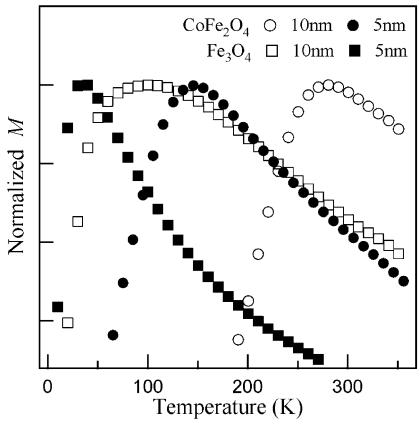

Figure 2. The zero-field-cooling magnetization of 5 and 10 nm Fe_3O_4 and the same sized $CoFe_2O_4$ nanocrystals under 100 Oe magnetic field.

for clearer viewing. The coercivity (H_C), saturation (M_S), and remanent (M_R) magnetizations as a function of the size of nanocrystals are shown in Figures 5, 6, and 7, respectively. Clearly, all these magnetic parameters of $CoFe_2O_4$ nanocrystals have higher values than those of the same sized Fe_3O_4 nanocrystals. The coercivity of $CoFe_2O_4$ nanocrystals is typically on the order of tens of thousands (Oe). Nevertheless it is in the range of only several hundreds oersted for Fe_3O_4 nanocrystals. For instance, the coercivity of 5 nm Fe_3O_4 nanocrystals is 214 Oe. However, 5 nm $CoFe_2O_4$ nanocrystals possess a coercivity of 10.8 kOe, which is more than 50 times higher than that of the Fe_3O_4 nanocrystals. As for the saturation and remanent magnetization, the trend for both of them is increased at first with increasing nanocrystal size. After a certain size, the saturation magnetization is flat and comparable to the values of bulk Fe_3O_4 and $CoFe_2O_4$ spinels, which have the saturation magnetization of 86−90 and 80 emu/g at room temperature,

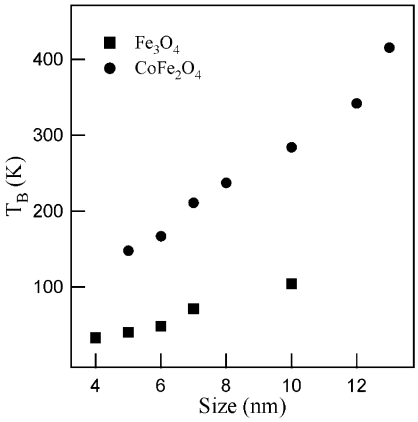

Figure 3. The blocking temperature vs the sizes of Fe_3O_4 and $CoFe_2O_4$ nanocrystals.

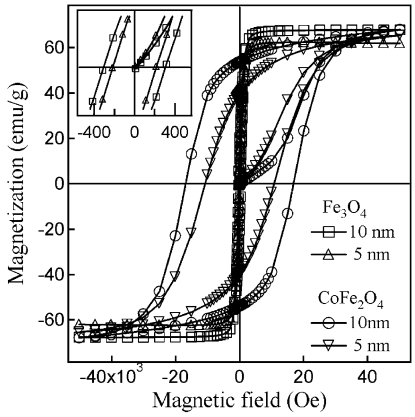

Figure 4. The field-dependent magnetization of 5 and 10 nm Fe_3O_4 and the same sized $CoFe_2O_4$ nanocrystals at 5 K. The insert shows the enlarged partial hysteresis curves for 5 and 10 nm Fe_3O_4 nanocrystals, respectively.

respectively.[21] An average 10 emu/g larger of M_S by $CoFe_2O_4$ nanocrystals is deduced when comparing to the same sized Fe_3O_4 nanocrystals.

At room temperature, $CoFe_2O_4$ and Fe_3O_4 nanocrystals with sizes of 5 and 10 nm clearly display the characteristic feature of a superparamagnetic state with the disappearance of coercivity (Figure 8), which is consistent with the fact that the blocking temperatures of all these nanocrystals are below room temperature. Also, the magnetization rises very rapidly with increasing strength of applied field. At about 1 T, the magnetization of these nanocrystals is already close to the saturation point.

The major factor for determining the superparamagnetic properties of nanocrystals is magnetocrystalline anisotropy. It originates from the spin−orbital (L−S) coupling at crystal lattices. According to Stoner−Wohlfarth single domain theory,[22] the magnetocrystalline anisotropy energy, E_A, of a single domain nanocrystal is approximated by

$$E_A = KV \sin^2 \theta \qquad (1)$$

where K is the magnetocrystalline anisotropy constant, V is the volume of nanocrystal, and θ is the angle between the ease axis of nanocrystal and the direction of field-induced magnetization. The magnetocrystalline anisotropy serves as an energy barrier to block the spin relaxation, which changes the magnetic state from ferromagnetic to superparamagnetic. The magnetic moment can be agitated into superparamagnetic relaxation by thermal energy (k_BT). The height of E_A determines the block temperature

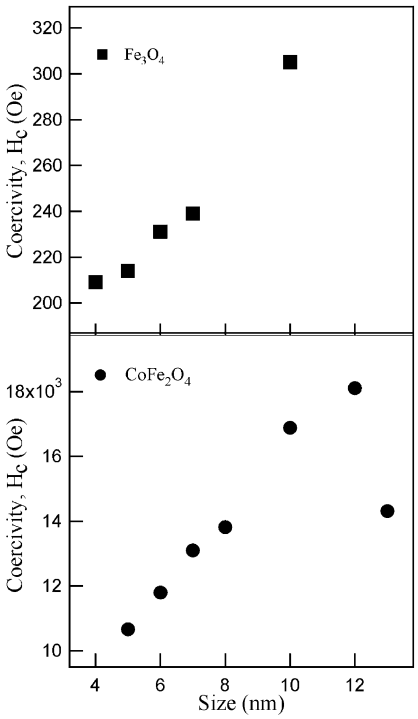

Figure 5. Coercivity vs sizes of Fe_3O_4 and $CoFe_2O_4$ nanocrystals.

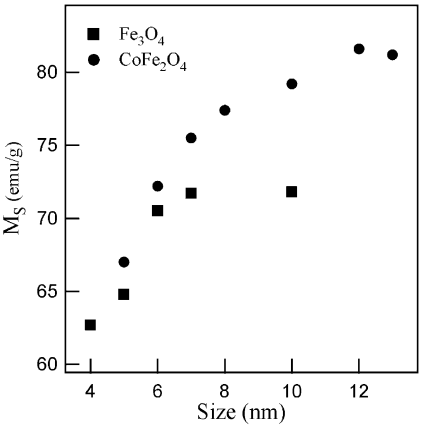

Figure 6. Saturation magnetization vs sizes of Fe_3O_4 and $CoFe_2O_4$ nanocrystals.

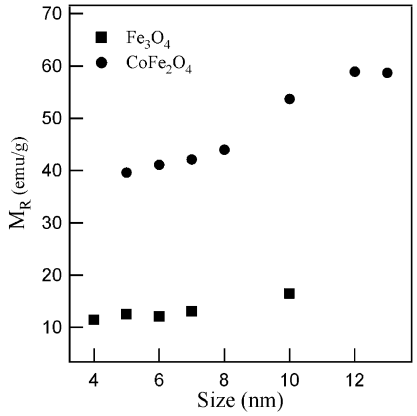

Figure 7. Remanence magnetization vs sizes of Fe_3O_4 and $CoFe_2O_4$ nanocrystals.

at which the thermal activation can overcome E_A and the nanocrystals transfer into the superparamagnetic state. Both the magnetocrystalline anisotropy constant K and the volume of nanocrystals control the magnetic anisotropy. The magnitude

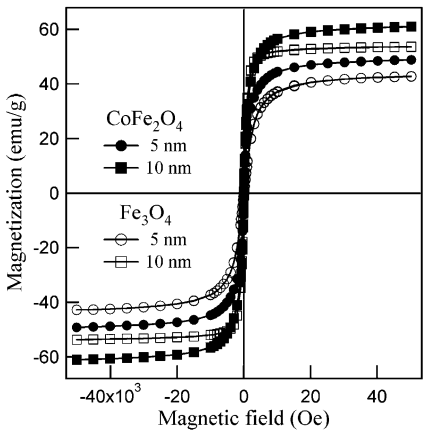

Figure 8. The field-dependent magnetization of 5 and 10 nm Fe_3O_4 and $CoFe_2O_4$ nanocrystals at 300 K.

of K is closely related to the strength of L−S coupling. As a result, the superparamagnetic properties of nanocrystals can be directly correlated with the variation of L−S coupling strength.

The single ion model has been successfully used in bulk magnetic materials to semiquantitatively evaluate the magnitude of anisotropy constant K.[23,24] The magnetic anisotropy is the result of the accumulative contribution of individual magnetic cations. In nanocrystals with a single magnetic domain structure, the possible complications from the domain wall pinning and movement do not exist. Therefore, the magnetic coupling at the individual lattice site can be straightforwardly correlated to magnetic properties such as superparamagnetism.

For a crystal with a cubic spinel structure, metal cations occupy the tetrahedral (A site) and octahedral (B site) lattice sites. Since the ligand field is weak in spinel ferrites, all cations assume high spin states. A Fe^{3+} cation with $3d^5$ electron configuration usually has its orbital angular momentum quenched in a weak ligand field. Therefore, the contribution to the magnetic anisotropy should only come from Co^{2+} and Fe^{2+} cations in $CoFe_2O_4$ and Fe_3O_4, respectively. The great difference in L−S coupling strength between Co^{2+} and Fe^{2+} determines the relative magnitude of magnetic anisotropy. Considering the ligand field at B sites, the $3d^6$ electron configuration of the Fe^{2+} cation gives a ground energy state of $^5T_{2g}$ under the O_h symmetry. However, this cubic symmetry is often lowered to a trigonal field in spinel due to the structural distortion from the Jahn−Teller effect and/or the nonstructural distortion from the interactions between the central cation and the cations outside the nearest neighborhood of the central ion. As a result, the triplet degenerated energy state of T_{2g} splits into two levels of E and B_2 with B_2 as the ground state.[23,24] The orbital angular momentum in an Fe^{2+} cation with a B_2 ground state is quenched and little spin−orbital coupling should be expected. A Co^{2+} cation with $3d^7$ electron configuration at a B site in $CoFe_2O_4$ has a triplet $^4T_{1g}$ ground state. Even though the trigonal field is introduced with the T_{1g} ground state further splitting into A_2 and E states, the Co^{2+} cation with a degenerated ground state of E is still considered to have a strong L−S coupling, and consequently contributes greatly to the magnetic anisotropy of $CoFe_2O_4$.[25−26]

The strong L−S couplings at Co^{2+} lattice sites surely will generate a large anisotropy constant K and result in much higher anisotropy energy barriers in $CoFe_2O_4$ nanocrystals than the same sized Fe_3O_4 nanocrystals. Hence, the observed higher blocking temperature of $CoFe_2O_4$ nanocrystals should not be a surprise, as shown in Figure 3. Although both types of nanocrystals have the energy barrier increased with increasing size, a larger K makes the increase in $CoFe_2O_4$ nanocrystals much steeper (eq 1). Consequently, the difference on the blocking temperature is increasingly larger as the size of nanocrystals increases (Figure 3).

The coercivity of magnetic nanocrystals is surely related to the magnetic anisotropy. At a given temperature, the required magnetic field strength for overcoming anisotropy to flip the magnetic spin certainly increases with increasing anisotropy energy barrier. Strong L−S couplings in Co^{2+} cations result in much higher coercivity in $CoFe_2O_4$ than Fe_3O_4 nanocrystals (Figure 4). The coercivity of nanocrystals also has a contribution from the surface anisotropy of nanocrystals.[27] The decrease in coercivity for the $CoFe_2O_4$ nanocrystals with a size above 12 nm probably results from the decrease of the surface anisotropy contribution since the surface becomes much less dominant with the growing size of the nanocrystals (Figure 5).

The great difference in superparamagnetic properties of the same sized $CoFe_2O_4$ and Fe_3O_4 nanocrystals surely facilitates our fundamental understanding of magnetism at the nanometer scale. $CoFe_2O_4$ nanocrystals clearly display better magnetic characteristics than Fe_3O_4 nanocrystals. For instance, larger saturation magnetization will reduce the requirement for the strength of the magnetic field to manipulate the nanocrystals. $CoFe_2O_4$ nanocrystals also show a rapid increase of magnetization responding to applied field even at relatively low field strength at room temperature (Figure 8). Although Fe_3O_4 nanocrystals display a similar response, the magnetization from $CoFe_2O_4$ nanocrystals is markedly enhanced. Clearly, the $CoFe_2O_4$ nanoparticulate system is a good candidate for biomedical applications in terms of magnetic characteristics. Certainly, their physiological feasibility needs to be systematically studied.

In summary, the systematic characterization and comparison of the superparamagnetic properties of cobalt ferrite and magnetite nanocrystals with similar sizes have been carried out. Compared to Fe_3O_4 nanocrystals, the same sized $CoFe_2O_4$ nanocrystals possess at least a 100 deg higher blocking temperature, over 50 times larger coercivity, and an average 10 emu/g enhancement in saturation magnetization. Strong electron spin−orbital coupling at Co^{2+} lattice sites leads to greater magnetic anisotropy, which in turn gives rise to such a dramatic discrepancy on magnetic properties between these two types of nanocrystals in the same spinel ferrites family. The study elucidates that it is possible to introduce the different metal cations to manipulate the strength of L−S coupling in spinel ferrite nanocrystals to precisely adjust the magnetic characters that are deemed crucial for the given applications. For instance, the nanocrystals have a much higher magnetization around the blocking temperature. The magnetic response of nanocrystals to an applied field can be greatly enhanced by adjusting the blocking temperature. Overall, this study shows that through fundamental studies magnetic nanoparticulate systems better than magnetite can be developed for biomedical applications such as magnetic cell sorting, DNA separation, and magnetic carriers for site-specific drug delivery.

Acknowledgment. All TEM studies were performed at the Electron Microscopy Center at Georgia Institute of Technology. This research is supported in part by Sandia National Laboratory and the PECASE program.

References and Notes

(1) Sun, S.; Murray, C. B.; Weller, D.; Folks, L.; Moser, A. *Science* **2000**, *287*, 1989.

(2) Puntes, V. F.; Krishnan, K. M.; Alivisatos, A. P. *Science* **2001**, *291*, 2115.
(3) Dumestre, F.; Chaudret, B.; Amiens, C.; Renaud, P.; Fejes, P. *Science* **2004**, *303*, 821.
(4) Olsvik, O.; Popovic, T.; Skjerve, E.; Cudjoe, K. S.; Hornes, E.; Ugelstad, J.; Uhlen, M. *Clin. Microbiol. Rev.* **1994**, *7*, 43.
(5) Haukanes, B. I.; Kvam, C. *Nat. Biotechnol.* **1993**, *11*, 60.
(6) Uhlen, M. *Nature* **1989**, *340*, 733.
(7) Berry, C. C.; Curtis, A. S. G. *J. Phys. D*: *Appl. Phys.* **2003**, *36*, R198.
(8) Mitchell, D. G. *J. Magn. Reson. Imaging* **1997**, *7*, 1.
(9) Weissleder, R.; Bogdanov, A.; Neuwelt, E. A.; Papisov, M. *Adv. Drug Delivery Rev.* **1995**, *16*, 321.
(10) Pankhurst, Q. A.; Connolly, J.; Jones, S. K.; Dobson, J. *J. Phys. D* **2003**, *36*, R167.
(11) Senyei, A.; Widder, K.; Czerlinski, G. *J. Appl. Phys.* **1978**, *49*, 3578.
(12) Lubbe, A. S.; Bergemann, C.; Brock, J.; McClure, D. G. *J. Magn. Magn. Mater*. **1999**, *194*, 149.
(13) Alexiou, C.; Arnold, W.; Klein, R. J.; Parak, F. G.; Hulin, P.; Bergemann, C.; Erhardt, W.; Wagenpfeil, S.; Lubbe, A. S. *Cancer Res*. **2000**, *60*, 6641.
(14) Nam, J.-M.; Thaxton, C. S.; Mirkin, C. A. *Science*, **2003**, *301*, 1884.
(15) Weissleder, R.; Kelly, K.; Sun, E. Y.; Shtatland, T.; Josephson, L. *Nat. Biotechnol*. **2005**, *23*, 1418.
(16) Rondinone, A. J.; Samia, A. C. S.; Zhang, Z. J. *J. Phys. Chem. B* **1999**, *103*, 6876.
(17) Liu, C.; Zou, B.; Rondinone, A. J.; Zhang, Z. J. *J. Am. Chem. Soc.* **2000**, *122*, 6263.
(18) Rondinone, A. J.; Liu, C.; Zhang, Z. J. *J. Phys. Chem. B* **2001**, *105*, 7967.
(19) Sun, S.; Zeng, H. *J. Am. Chem. Soc.* **2002**, *124*, 8204.
(20) Song, Q.; Zhang, Z. J. *J. Am. Chem. Soc.* **2004**, *126*, 6164.
(21) Wohlfarth, E. P.; Ed. *Ferromagnetic Materials*; Elsevier: Amsterdam, The Netherlands, 1982; Vol. 3, p 296.
(22) Stoner, E. C.; Wohlfarth, E. P. *Trans. R. Soc.* **1948**, *A240*, 599;.
(23) Yosida, K.; Tachiki, M. *Prog. Theor. Phys*. **1957**, *17*, 331.
(24) Wolf, W. P. *Phys. Rev*. **1957**, *108*, 1152.
(25) Slonczewski, J. C. *Phys. Rev*. **1958**, *110*, 1341.
(26) Baltzer, P. K. *J. Phys. Soc. Jpn*. **1962**, *17* (Suppl.), 192.
(27) Vestal, C. R.; Zhang, Z. J. *J. Am. Chem. Soc*. **2003**, *125*, 9828.